7th International Building Physics Conference

# IBPC2018

## Proceedings

**SYRACUSE, NY, USA**

September 23 - 26, 2018

Healthy, Intelligent and Resilient
Buildings and Urban Environments

ibpc2018.org | #ibpc2018

# Using rain and vegetation to improve thermal comfort in a hot street canyon with fully-integrated urban climate modeling

Aytaç Kubilay[1,*], Jan Carmeliet[1,2] and Dominique Derome[1]

[1]Laboratory of Multiscale Studies in Building Physics, Empa, 8600 Dübendorf, Switzerland
[2]Chair of Building Physics, ETH Zurich, 8092 Zürich, Switzerland

[*]*Corresponding email: aytac.kubilay@empa.ch*

## ABSTRACT
Building materials that are commonly used in urban areas generally have higher sensible heat storage and radiation entrapment, while having lower moisture storage and evapotranspiration, in comparison to the materials found in rural areas. These differences play a significant role in the occurrence of the urban heat island (UHI) effect, which has adverse impacts on thermal comfort, energy use and public health. Coupled numerical simulations of computational fluid dynamics (CFD) with the heat and mass transfer (HAM) in porous urban materials are performed to estimate the evaporative-cooling potential of different pavements in a street canyon. The local thermal comfort following a rain event on different pavements is compared with the one in presence of a grass-covered surface. The results show that the grass-covered ground provides better pedestrian thermal comfort, followed by porous material with large liquid permeability.

## KEYWORDS
Urban climate, Thermal comfort, Computational fluid dynamics, Porous media, Vegetation

## INTRODUCTION
Pedestrian thermal comfort is influenced by mean radiant temperature and local parameters such as air temperature, relative humidity and wind speed. Urban areas generally have increased sensible heat storage and radiation entrapment while having a decreased amount of evapotranspiration. Therefore, urban materials strongly influence the outdoor thermal comfort. The present study aims to investigate the evaporative-cooling potential of various urban pavement materials, showing different thermal and moisture transport properties.

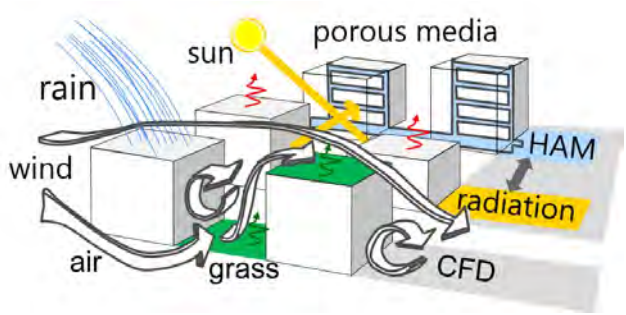


Figure 1. Schematic of the main physics implemented in the coupled urban microclimate model (CFD: Computational fluid dynamics, HAM: Heat and moisture transport).

A fully-integrated urban microclimate model is developed, where CFD simulations of wind flow around buildings are coupled with the heat and mass transport (HAM) in porous urban materials. The model solves for wind flow, transport of heat and humidity in the air and

transport of heat and moisture in building materials (Fig 1). Solar (short-wave) and thermal (long-wave) radiative heat exchange between surfaces and the sky are taken into account with multiple with diffuse reflections. Surface wetting due to wind-driven rain (WDR) is calculated based on an Eulerian multiphase model.

The proposed model is applied on a street canyon, where the three-dimensional heat and mass transport within the street-canyon ground and facades is coupled with the wind flow. The study at local scale (< 100 m) allows for parametric studies, where different contributions to thermal comfort can be evaluated in detail, such as shading, convective cooling, sensible heat transfer due to rain and evaporation. Detailed temporal and spatial analyses can be performed. The present study focuses on the drying period of different porous urban materials following a rain event. The impact of drying of pavement materials on outdoor thermal comfort is compared with the impact of evapotranspiration from a grass-covered surface. The thermal comfort for pedestrians is evaluated using the Universal Thermal Climate Index (UTCI) (Fiala et al. 2001). UTCI provides the perceived temperature based on surface temperatures, air temperature, relative humidity and wind speed.

## NUMERICAL MODEL AND METHODOLOGY

### Governing equations

The wind flow is solved using 3D steady Reynolds-averaged Navier-Stokes (RANS) with the standard $k$-$\varepsilon$ model. Additionally, transport equations for heat and moisture are solved. Heat is considered as an active scalar, where buoyancy is modeled by using a compressible formulation of the Navier-Stokes equations and calculating air density based on ideal gas law instead of the Boussinesq approximation. Moisture is modeled as a passive scalar, where the transported quantity is the humidity ratio, i.e. ratio of the mass of water vapor to the mass of dry air. Grass is modeled as a porous zone, providing the source/sink terms for heat, moisture and momentum (Manickathan et al. 2018a). Transpiration from grass blades is calculated based on leaf stomata resistance. Grass leaf temperature is calculated with an iterative energy balance calculation based on latent and sensible heat fluxes (Manickathan et al. 2018b).

Absorption, transport and storage of heat and moisture are simulated within the building materials using coupled heat and moisture transport equations for porous media. The present study uses the continuum modeling approach, where the different phases are not distinguished separately at a certain point in the material but, instead, the macroscopic behavior of the porous material is modeled. Within porous urban materials, the coupled heat and moisture transport equations are solved (Janssen et al, 2007):

$$(c_0\rho_0 + c_l w)\frac{\partial T}{\partial t} + \left(c_l T \frac{\partial w}{\partial p_c}\right)\frac{\partial p_c}{\partial t} = -\nabla(q_c + q_a) \tag{1}$$

$$\frac{\partial w}{\partial p_c}\frac{\partial p_c}{\partial t} = -\nabla(g_l + g_v) \tag{2}$$

where $w$ denotes moisture content, $p_c$ capillary pressure, $c_0$ specific heat of dry material, $\rho_0$ density of dry material, $c_l$ the specific heat of liquid water, $T$ absolute temperature. The fluxes $q_c$ and $q_a$ denote conductive and advective heat transfer, whereas $g_l$ and $g_v$ denote liquid and vapor moisture transfer including latent heat. The moisture exchange at the exterior surfaces of building materials comprises the rain flux and the convective vapor exchange, whereas the heat exchange comprises the convective heat transfer, the radiative heat transfer, the sensible

heat transfer due to rain and the latent and sensible heat transfer due to vapor exchange. Wetting due to rain on each surface in the computational domain is predicted using an Eulerian multiphase model (Kubilay et al. 2014), which solves for different sizes of raindrops and calculates the WDR intensity.

Solar and thermal radiative fluxes are calculated with separate systems of linear equations based on a radiosity approach. The direct component of incoming solar radiation is calculated with ray tracing. Multiple reflections of both solar and thermal radiation are calculated using view factors, which are calculated based on algebraic relations between surfaces. All building surfaces are assumed to be opaque to both longwave and shortwave radiation. The model further assumes that the building surfaces are grey, i.e. emissivity and absorptivity are equal and independent of wavelength. Absorption of solar radiation within the grass zone is modeled based on the Beer-Lambert law.

The numerical multi-transport model is implemented into OpenFOAM. The general framework and the detailed methodology of the model were given in an earlier paper (Kubilay et al. 2017).

**Coupling algorithm**

The coupling between the air and porous domains is performed by sequentially solving the steady RANS equations in the air and the unsteady heat and moisture transfer in porous building materials. This approach is valid due to the fact that the time scale of transport in building materials is larger than the time scale of transport in air. For the air domain, Dirichlet boundary conditions are used, where the values for temperature and humidity ratio are defined at the coupled boundaries. For the porous domains, Neumann boundary conditions are used, where the heat and moisture fluxes are defined at the material surfaces.

Transient heat and mass transport in porous domains are simulated using adaptive time steps (Janssen et al. 2007), during which the solution of the air domain remains constant. At each time step, internal iterations between heat and moisture equations are performed until temperature and moisture content values converge, while the thermal radiative heat fluxes are updated accordingly. Finally, the new values for temperature and moisture at the solid boundaries are used to solve the steady air flow for the next exchange time step. This information exchange between domains is repeated at each exchange time step (Saneinejad et al. 2014). In this study, an exchange time step of 10 min is chosen. For a more detailed description of the model, the reader is referred to Kubilay et al. (2017).

## DESCRIPTION OF THE CASE STUDY

The case study is performed on an isolated three-dimensional street canyon, which is composed of two buildings with flat facades and horizontal roofs with a north-south orientation. Both buildings have the dimensions of height × length × width of $10\times10\times50$ m$^3$. The computational domain is shown in Fig 2 as well as the orientation of the street canyon with respect to the wind direction and sun. For simplicity, wind speed is assumed constant at 5 m/s at the building height and wind direction is assumed perpendicular to the street canyon, i.e. from west. The variation of ambient temperature and total solar radiation intensity are based on June 21$^{st}$, a typical early summer day with moderate ambient temperatures in Zurich, Switzerland. The ambient temperature varies between 11°C and 19°C, while the relative humidity (RH) varies between 62% and 86%. The simulations are run for several days with 'dry' conditions with no rain event until the conditions reach a daily thermal cycle that is

independent from the initial values. For 'rainy' conditions, a rain event of 1 mm/h intensity is applied for a duration of 10 hours at nighttime.

The leeward and windward facades of the street canyon are finished with an exterior layer of brick masonry with a thickness of 0.09 m. For the outer layer of the street-canyon ground, which has a thickness of 0.10 m, different materials are considered: concrete, soil and brick. Beneath this layer, an additional soil layer with a depth of 1.90 m is present for each case. Thermal properties for the dry materials are given in Table 1. For the simulations with grass, no rain event is modeled, however, transpiration rate is calculated based on the assumption that enough moisture is available in the soil at all times. Grass blades of 10 cm height are considered on the street-canyon ground (soil). Leaf area intensity (LAI) is taken as 2 and leaf drag coefficient as 0.2.

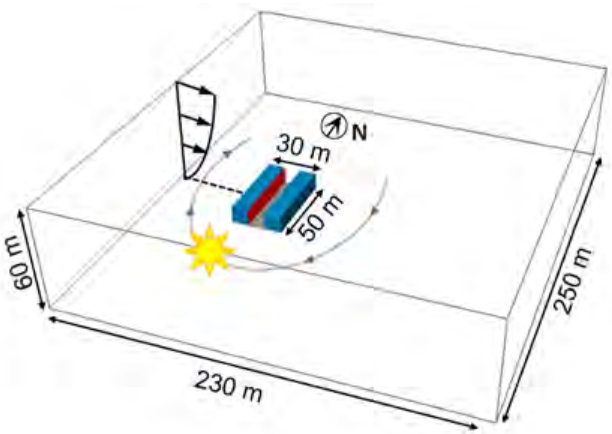


Figure 2. Computational domain and orientation of the street canyon with respect to wind direction and sun trajectory.

Table 1. Thermal properties of the dry porous media.

| Material | Density [kg/m3] | Specific heat [J/kgK] | Thermal conductivity [W/mK] |
|---|---|---|---|
| Bare soil | 1150 | 650 | 1.500 |
| Concrete | 2280 | 800 | 1.500 |
| Clay brick | 1600 | 1000 | 0.682 |

**RESULTS**

Fig 3 compares the surface temperature at the center of the street-canyon ground for a duration of two days. Before the rain event, the surface temperatures for bare soil, concrete and clay brick reflect the thermal diffusivity and specific heat of the respective materials. After the rain event, due to evaporation, the maximum surface temperature decreases as much as 20°C for brick and 15°C for soil. A slightly larger reduction of temperature is observed for brick than for soil as the brick is capillary active and has a larger liquid permeability than soil in this case. For concrete, the decrease in maximum temperature is negligible as a much smaller amount of water is absorbed in concrete. Grass-covered soil temperature is in general at around the same values as concrete as it is shaded by grass, while the maximum grass leaf temperature is 26°C as a result of latent heat due to evaporation.

Fig 4 compares the conditions at pedestrian height (1.75 m) at the center of the street canyon, namely the air temperature, air relative humidity and the UTCI. Before the rain event, as a result of evapotranspiration, the lowest air temperature and the highest relative humidity are

observed for grass-covered street canyon. After the rain event, air temperature decreases by up to 1.4°C for brick. However, simultaneously, a considerable increase of relative humidity is observed as shown in Fig. 4(b). Overall, the lowest UTCI is observed for grass (Fig. 4(c)). The decrease in UTCI due to rain event is up to 2.0°C.

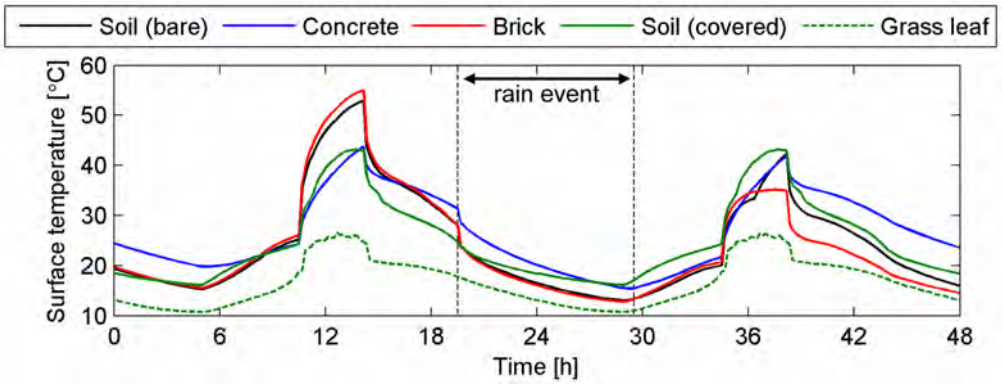


Figure 3. Variation of surface temperature at the center of the street-canyon ground for different materials.

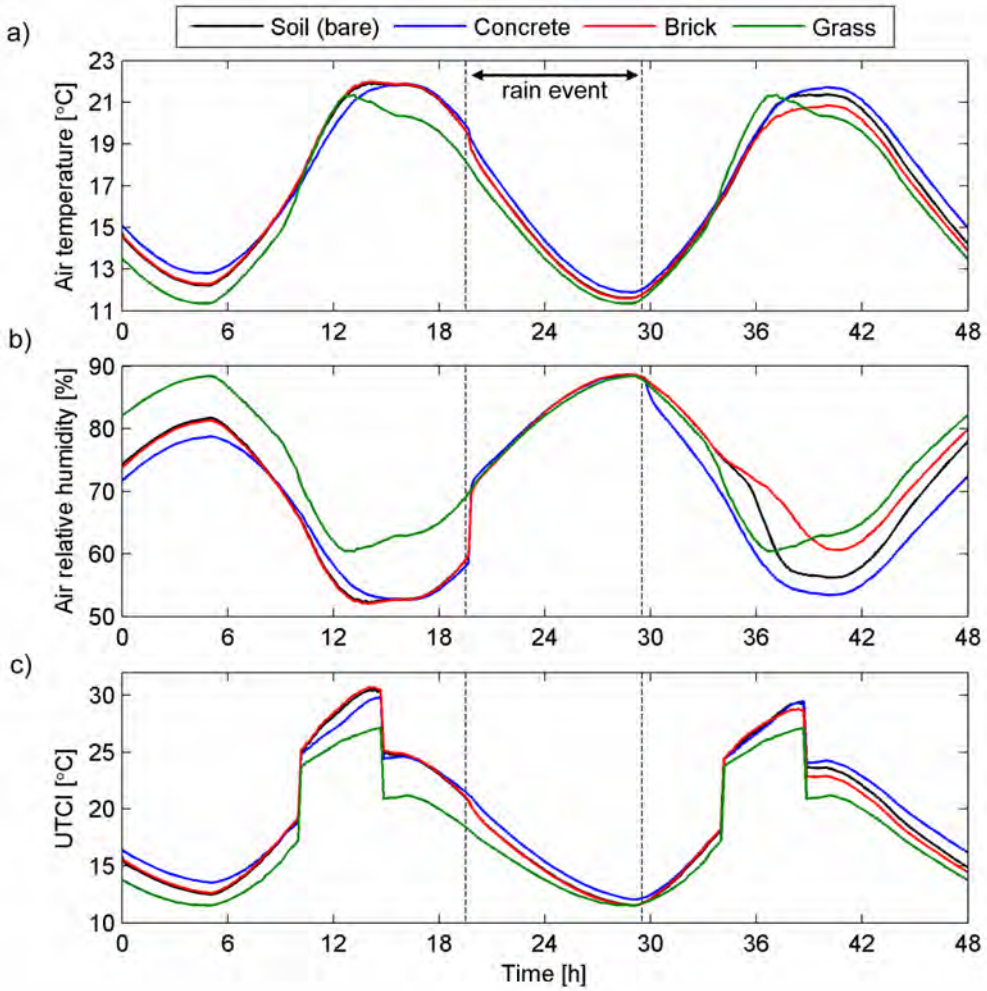


Figure 4. Variation of a) air temperature, b) air relative humidity and c) UTCI at pedestrian height at the center of the street canyon.

## DISCUSSION AND CONCLUSIONS

The influence of different porous urban materials exposed to environmental loading is investigated. Evaporative-cooling potential for the materials is compared to the conditions provided by the grass-covered area. While the results obtained for the isolated street canyon cannot be generalized for complete range of urban areas, the study indicates several significant results. It is found that the effect of transpirative cooling due to grass is apparent both in terms of air temperature and of UTCI. While, the increase in relative humidity has an adverse effect on thermal comfort, overall, improved conditions are observed for the grass-covered surface. The evaporative-cooling effect due to the absorption and evaporation of rain water in porous urban materials increases as the liquid permeability of materials gets larger. We note that the conclusions depend on several factors such as total wetting amount due to rain, wetting period of the day, leaf area intensity of grass and local wind flow conditions. The transpiration from grass is also dependent on the water availability in the soil. Further work is planned on including on evaluating the local effects of heat waves, at neighborhood scale.

## ACKNOWLEDGEMENT

The support through the Swiss Competence Center for Energy Research project ‘‘Future Energy Efficient Buildings and Districts’’, CTI.1155000149, is gratefully acknowledged.

## REFERENCES

Fiala D., Lomas K. J., Stohrer M. 2001. Computer prediction of human thermoregulatory and temperature responses to a wide range of environmental conditions. *International Journal of Biometeorology*, 45(3):143–159.

Janssen H., Blocken B., Carmeliet J. 2007. Conservative modelling of the moisture and heat transfer in building components under atmospheric excitation. *International Journal of Heat and Mass Transfer*, 50:1128-1140.

Kubilay A., Derome D., Blocken B., Carmeliet J. 2014. Numerical simulations of wind-driven rain on an array of low-rise cubic buildings and validation by field measurements. *Building and Environment*, 81:283-295.

Kubilay A., Derome D., Carmeliet J. 2017. Coupling of physical phenomena in urban microclimate: A model integrating air flow, wind-driven rain, radiation and transport in building materials. *Urban Climate*. In press.

Manickathan L., Defraeye T., Allegrini J., Derome D., Carmeliet J. 2018a. Parametric study of the influence of environmental factors and tree properties on the transpirative cooling effect of trees. *Agricultural and Forest Meteorology*, 248:259-274.

Manickathan L., Kubilay A., Defraeye T., Allegrini J., Derome D., Carmeliet J. 2018b. Influence of vegetation on pedestrian thermal comfort in a street canyon, In: *Proceedings of 1st International Conference on New Horizons in Green Civil Engineering (NHICE-01)*, Victoria, BC, Canada, April 25 – 27.

Saneinejad S., Moonen P., Carmeliet J. 2014. Coupled CFD, radiation and porous media model for evaluating the micro-climate in an urban environment. *Journal of Wind Engineering and Industrial Aerodynamics*, 128:1-11.